

See discussions, stats, and author profiles for this publication at: <https://www.researchgate.net/publication/232740227>

Solvent Polarity-Induced Conformational Unlocking of Asparagine

ARTICLE *in* THE JOURNAL OF PHYSICAL CHEMISTRY A · OCTOBER 2012

Impact Factor: 2.69 · DOI: 10.1021/jp307715n · Source: PubMed

CITATIONS

3

READS

17

3 AUTHORS:



Ananda Rama Krishnan Selvaraj

16 PUBLICATIONS 121 CITATIONS

SEE PROFILE



Natarajan Arul Murugan

KTH Royal Institute of Technology

72 PUBLICATIONS 574 CITATIONS

SEE PROFILE



Hans Agren

KTH Royal Institute of Technology

867 PUBLICATIONS 18,728 CITATIONS

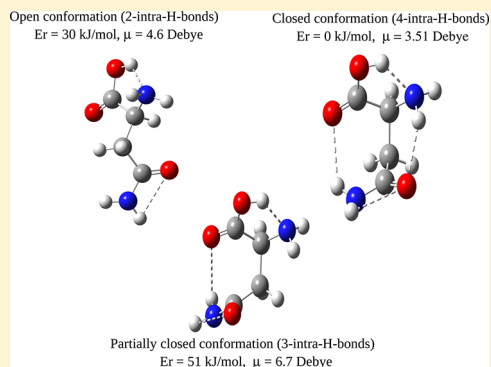
SEE PROFILE

1 Solvent Polarity-Induced Conformational Unlocking of Asparagine

2 Ananda Rama Krishnan Selvaraj, N. Arul Murugan, and Hans Ågren*

3 Division of Theoretical Chemistry and Biology School of Biotechnology, Royal Institute of Technology, SE-10691 Stockholm,
4 Sweden5 **S** Supporting Information

ABSTRACT: Classical and Car–Parrinello molecular dynamics simulations are performed to study the effects of different solvents on the conformational distribution of asparagine. Conformational populations obtained from the simulations in gas phase and in nonpolar chloroform solvent are in agreement with the most probable single conformation of asparagine in the gas phase measured in recent laser ablation with molecular beam Fourier transform microwave spectroscopy experiments. We rationalize that intramolecular hydrogen bonding and dipole–dipole interactions between carbonyl groups dictate such a conformational locking to a single asparagine conformer. The solvent polarity induced interlocking or intermolecular hydrogen bonding with water solvent molecules destabilizes the (NH···O=C) bonding between side chain and terminal groups of asparagine, while not essentially affecting the (NH···O=C) intramolecular hydrogen bondings within the side chain as well as with in the terminal groups. Such a conformational unlocking or cage effect is observed in asparagine within aqueous solution. We observed a spontaneous conversion of neutral to zwitterionic isomer of asparagine in aqueous solution, which is in agreement with interpretation of Raman spectroscopy results. Using Møller–Plesset second order perturbation theory, we show that a crossover from neutral to zwitterionic tautomeric shift occurs on asparagine in between DMSO and water solvents. The ramification of these findings for the conformational character of asparagine is briefly discussed.



1. INTRODUCTION

Asparagine is not among the essential amino acids though it plays a critical role in biological systems due to its deamination characteristics. Its deamination tendency is a spontaneous biological process, which is responsible for protein degradation and aging. It also serves as a molecular clock in biological systems.^{1–24} There are several experimental reports that discuss the conformational distribution of asparagine in the gas phase. Fourier transform infrared (FT-IR) spectroscopy and laser ablation with molecular beam Fourier transform microwave spectroscopy (LA-MB-FTMW) investigations have been carried out on asparagine showing the presence of a probable single conformation of asparagine in the gas phase.^{25,26} A most probable closed conformation with four major intramolecular hydrogen bonds has been identified from conformational search and optimizations within Møller–Plesset (MP2) level of theory, which supports experimental findings.^{25,26} This is a rather striking observation considering the fact that amino acids are known to exist in numerous conformations. Moreover, the presence of a neutral isomer in gas phase^{25,26} and zwitterionic isomer in the solid state and aqueous solution of asparagine has been reported by Raman spectroscopy.^{27,28} We here intend to investigate the reason behind such conformational preference in asparagine in the gas phase and the interaction between asparagine and solvent molecules in terms of cage effects. Thus, the current study aims at addressing the effects of solvent polarity on the conformational locking in asparagine, which will be complementary to recent gas phase, solid, and solution

phase experimental works on asparagine.^{27,28} We also highlight earlier Hartree–Fock and density functional theory calculations performed on conformational properties, free energy calculations, and modeling of reaction mechanisms of the deamination process including cyclic succinimide intermediate formation in asparagine.^{29–42}

Since the conformational transitions usually are large time scale processes, we have carried out classical molecular dynamics (MD) simulations up to a few tens of nanoseconds. Asparagine has been studied in three different environments such as gas phase and nonpolar and polar solvents. The conformational states of asparagine can be characterized by analysis of the intramolecular hydrogen bonding. Therefore, all possible hydrogen bonds in asparagine were analyzed and compared with spectroscopic results, and the influence of solvent polarity on intramolecular hydrogen bonding is discussed. The locked or open conformation of asparagine is completely determined by its intramolecular hydrogen bondings and interactions between its polar carbonyl groups.⁴³ The structure of asparagine is given in Figure 1 with definition of torsion angles and terminal and side chain functional groups including atom numbering. One-fold potential energy surface scans were calculated at the MP2 level of theory on defined torsional angles to estimate all possible intramolecular

Received: August 3, 2012

Revised: October 27, 2012

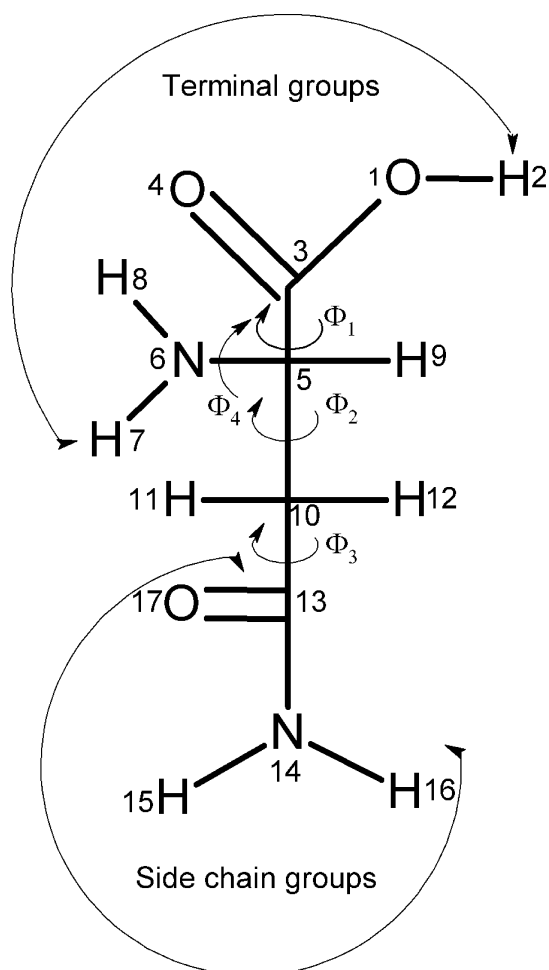


Figure 1. Molecular structure of asparagine with definition of torsion angles and atom numbering.

moments, which are dynamical quantities that evolve in time and depend on the chemical state of asparagine in instantaneous solvent environments. In addition to that, to understand the relationship between the dielectric values and shift toward zwitterionic isomer in asparagine, we have performed static calculations at the MP2 level on neutral, zwitterionic, and transition states of asparagine in different solvents where the solvents are described using a polarizable continuum model (PCM). We have studied the effect of solvent polarity on the energetics of these three states of asparagine.

2. COMPUTATIONAL DETAILS

Classical atomistic MD simulations were performed with the AMBER11 program.⁴⁴ Simulations were performed on asparagine in vacuum and in two different solvent environments such as water and chloroform. The atomic charges for the asparagine were adopted from the best fitting to reproduce electrostatic potential obtained from HF/6-31G* level calculations using the CHELPG procedure⁴⁵ as implemented in the Gaussian09 software.⁴⁶ We have employed the GAFF force-field for asparagine as the applicability of this force field to model the structural and dynamical properties of organic molecules have been demonstrated in many earlier research reports.^{47–54} Moreover, a GAFF force-field for chloroform and TIP3P model for water were used in these simulations. The MD simulations were carried out in an orthorhombic box containing asparagine and solvents. Around 5812 water molecules and 1224 chloroform molecules were considered for two different solvents. Both types of MD simulations were performed for a total time scale of 10 ns with a 1 fs time step for integration of equation of motion. We have employed a cutoff of 10 Å for calculating nonbonded interactions within the solute–solvent systems. The MD simulations on the isolated asparagine were performed in vacuum with a total simulation time of 2 ns with a 1 fs time step. CPMD simulations were performed for the asparagine in two solvents using the CPMD/Gromos software.^{55–59} The initial structure for the solute–solvent systems in CPMD runs has been taken from the above-described classical MD run. In this set of calculations, the asparagine was considered to be in the QM region and the solvents are described using a molecular mechanics force-field. The QM description refers to the BLYP gradient-corrected functional level.^{60,61} The wave function for asparagine is based on plane wave basis sets, while Troullier–Martins⁶² pseudopotentials were adopted for various atoms in the CPMD run. The time step for integration of the Lagrangian equation of motion was kept as 0.125 fs (5 atomic units), and the total time scale for such CPMD simulations was approximately 5 ps. The classical MD and CPMD simulations were performed at 300 K temperature in an NPT ensemble. The final 2 ns of MD run trajectories and 2 ps trajectories of the CPMD simulations were considered for the analysis of intramolecular hydrogen bonding and end to end distance distribution.

For the calculation of intramolecular hydrogen bonding, a distance value of <3 Å has been used. A contact between a hydrogen bonding donor and acceptor with this distance criteria has been used as an indicator for formation of intramolecular hydrogen bonding. The conformational flexibility and polarity of asparagine are obtained with one-fold potential energy scans around the C–C and C–N bonds. We considered four such possibilities in asparagine, namely, those described by using torsion angles Φ_1 , Φ_2 , Φ_3 , and Φ_4 .

interactions and the conformational flexibility. The dependency of the dipole moment with respect to the torsion angles is shown to explain the effect of intramolecular hydrogen bonding on polarity.

Another important aspect for analyzing amino acids is their protonation state, which highly depends on solvent polarity and pH value of the solvent environment.^{16–24} Particularly, such proton transfer significantly influences the electron transfer process in many biological systems. Similarly, deamination process in asparagine-related proteins is also induced by proton transfer in aqueous solution because proton transfer forms planar α -carbanion and changes the molecular length of asparagine as well as creates different hydrogen bonding pattern. In aqueous solution, proton transfer from the terminal carboxyl group to the amino group results in a zwitterion of asparagine, which is known as amphiprotic nature of amino acids. Basically, the dynamic equilibrium between neutral and zwitterion does exist at an isoelectric point of any amino acids. The tautomeric shift toward either the neutral or zwitterionic isomers depends on solvent polarity and pH. We also show solvent effects on the crossover between isomers of asparagine. Classical molecular dynamics and hybrid QM/MM Car–Parrinello molecular dynamics (CPMD) simulations were used to study the solvent effects in asparagine. We have also followed the conformation and solvent-dependent polar nature of asparagine using the calculated D-RESP charges and dipole

Table 1. Intramolecular Hydrogen Bonding Distribution of Asparagine in Vacuum (V), Chloroform (C), and in Water (W) by CPMD and MD Simulations (Values Were Given As Percentage)

hydrogen bonding pair	CPMD(V)	MD(V)	CPMD(C)	MD(C)	CPMD(W)	MD(W)
(1) N(14)–H(16)···O(4)	0.00	79.20	19.71	47.91	3.72	2.15
(2) N(14)–H(15)···O(4)	92.19	0.00	0.00	0.00	0.00	0.00
(3) N(14)–H(15)···O(17)	100.00	100.00	100.00	100.00	100.00	100.00
(4) N(14)–H(16)···O(17)	0.00	23.70	0.00	18.72	0.00	12.75
(5) N(6)–H(7)···O(17)	91.00	99.25	0.00	96.59	0.00	0.00
(6) N(6)–H(8)···O(17)	0.00	6.85	98.34	6.70	0.00	0.00
(7) O(1)–H(2)···N(6)	100.00	100.00	100.00	99.89	100.00	77.28
(8) O(1)–H(2)···N(14)	0.00	0.00	0.00	0.00	0.00	0.00
(9) O(1)–H(2)···O(17)	0.00	0.85	0.50	4.78	0.00	4.65

Moreover, the energetics of neutral, transition state, and zwitterionic isomers of asparagine were studied in six different solvent environments. The solvent environment in the static calculations was considered implicitly using the polarizable continuum model. The rotational barriers and optimization of neutral, transition state, and zwitterionic isomers in different solvents were carried out using MP2 perturbation theory with a 6-31G(d,p) basis set⁶³ within the Gaussian09 program. The transition states of asparagine in different solvents were calculated by the synchronous transit-guided quasi-Newton (STQN) methodology.^{64,65}

3. RESULTS AND DISCUSSION

3.1. Solvent-Dependent Conformational Distribution of Asparagine. The conformational distribution of asparagine is dictated by various intramolecular and intermolecular hydrogen bondings. Therefore, we characterize the geometry of asparagine by analyzing different intramolecular hydrogen bonding patterns. All possible intramolecular hydrogen bonding pairs were considered in the analysis. There are nine such hydrogen bondings possible in asparagine. The first set of hydrogen bonding pairs in between terminal carboxyl and side chain amino groups are H(16)···O(4), H(15)···O(4), and H(2)···N(14) (for numbering of atoms, see Figure 1). Another set of hydrogen bonding pairs are H(15)···O(17), H(16)···O(17), and H(2)···N(6) contacts. In these pairs, two sets of hydrogen bondings can occur in between the side chain carbonyl and the amino groups and in between the terminal carboxyl and the amino groups, respectively. The remaining possible hydrogen bonding pairs are H(2)···O(17), H(7)···O(17), and H(8)···O(17). In that, the terminal carboxyl and amino groups are involved in the hydrogen bonding with side chain carbonyl groups, respectively. The percentage population of these intramolecular hydrogen bondings in asparagine calculated using CPMD and MD trajectories are presented in Table 1. The results show that the population of hydrogen bonding between terminal and side chain groups decreases with increasing solvent polarity. Particularly, the population of hydrogen bonding labeled as H(16)···O(4) decreases from 79.2% in vacuum to 2.15% in aqueous solution. This particular hydrogen bonding is necessary to observe the closed conformer in asparagine, which is drastically affected by the solvent polarity. This intramolecular hydrogen bonding distance in gas, chloroform, and aqueous solutions is shown in Figure 2, as a function of MD simulation time. The figure shows a diminishing trend of hydrogen bonding with increasing solvent polarity. This can be rationalized that, in an aqueous solution, there is also the possibility for intermolecular hydrogen bonding between the polar groups of asparagine

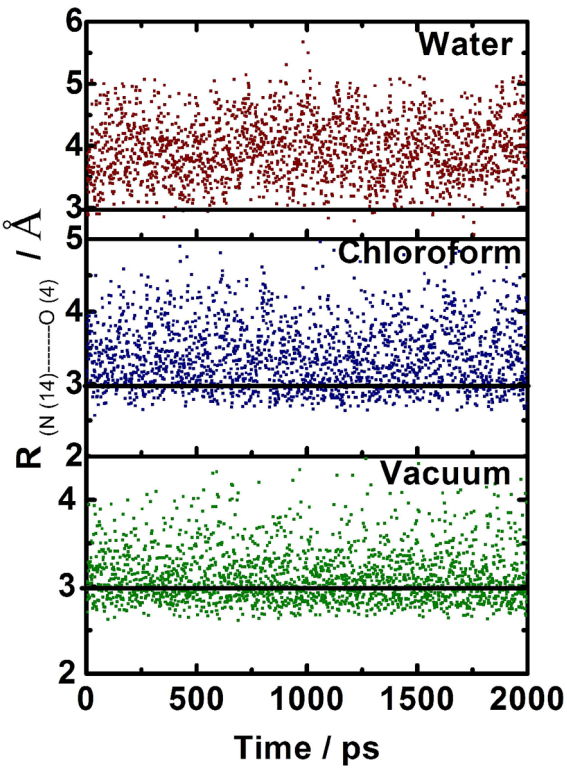


Figure 2. N(14)–H(16)–O(4) intramolecular hydrogen bonding distribution calculated from MD simulations in vacuum, chloroform, and water solvents (in each plot, a solid line at 3 Å shows the cutoff value of intramolecular hydrogen bonding).

with water solvent molecules in aqueous solution. This could be explained in terms of a cage-effect of asparagine in aqueous solution. In gas phase and chloroform solvent, the stabilization of asparagine only occurs through intramolecular hydrogen bonding, and therefore, the population of a closed conformer with four intramolecular hydrogen bonding appears to be the dominant one. However, the competing intra- and intermolecular hydrogen bonding for asparagine in aqueous solution also results in the population of several open conformers in the case of aqueous solution. Independent of solvent polarity, a high population of hydrogen bonding is observed within terminal groups and side chain groups, which are referred as N(14)–H(15)···O(17) and O(1)–H(2)···N(6) pairs. According to results in Table 1, a significant level of intramolecular hydrogen bonding between terminal amino and side chain carbonyl groups is found in vacuum and chloroform solvent, which is not observed in aqueous solution as can be seen from the values of pairs N(6)–H(7)···O(17) and N(6)–

H(8)⋯O(17). Overall, in the gas phase, the amount of intramolecular hydrogen bonding is higher in comparison to chloroform and aqueous solution. Thus, the locked or closed isomer is stabilized by four major intramolecular hydrogen bondings in the gas phase. This gas phase result is in agreement with recent gas phase FTMW experiment.^{25,26}

We observed two and three major intramolecular hydrogen bondings in water and chloroform solvents, respectively. The percentage of intramolecular hydrogen bonding decreases with increasing solvent polarity. The conformational locking in molecules like asparagine is not only controlled by intramolecular hydrogen bonding but is also stabilized by strong dipole–dipole interactions between two opposing carbonyl groups, as reported earlier.^{29–42} The distance between partially opposite charged atoms O17, C3 and O4, C13 of two different carbonyl groups were calculated and their normalized distributions are shown in Figures 3 and 4. The opposite

were calculated between reference atoms N14 and C3, and their normalized distribution curves are shown in Figure 5. The

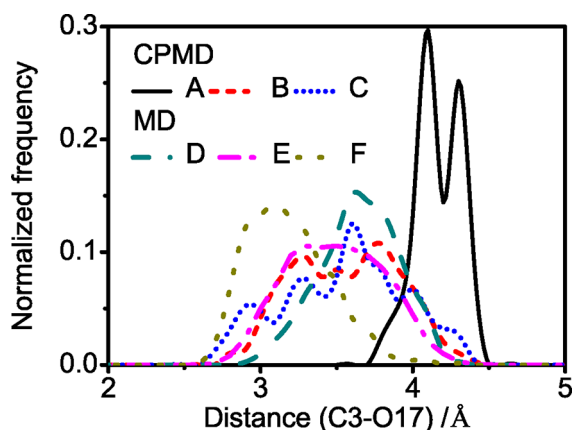


Figure 3. Distance between opposite charged atoms O17 and C3 in the carbonyl groups (A, vacuum; B, chloroform; C, water; D, vacuum; E, chloroform; F, water).

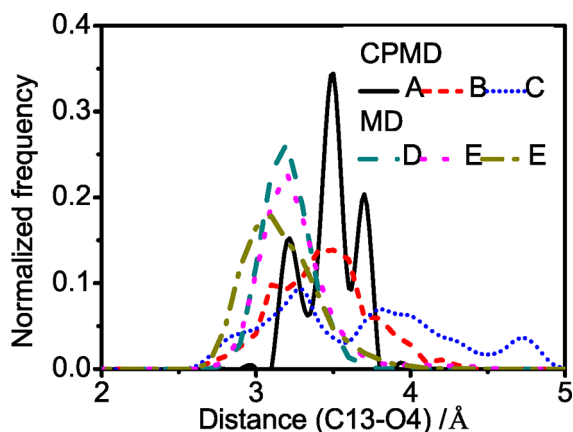


Figure 4. Distance between opposite charged atoms O4 and C13 in the carbonyl groups (A, vacuum; B, chloroform; C, water; D, vacuum; E, chloroform; F, water).

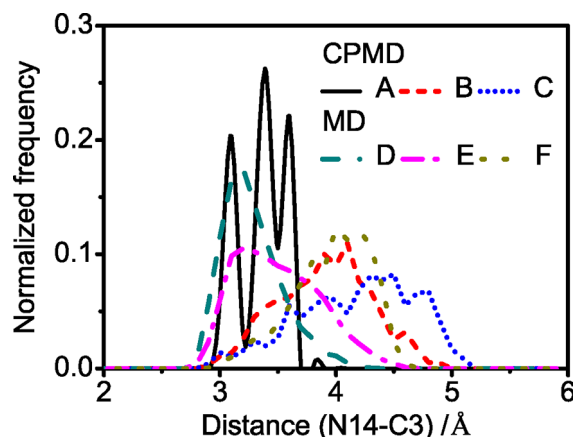


Figure 5. End to end distance values between N14 and C3 atoms (A, vacuum; B, chloroform; C, water; D, vacuum; E, chloroform; F, water).

average end to end distance values for asparagine are smaller in chloroform solvent than in aqueous solution, and for the gas phase, it is minimum. This trend is highly pronounced in MD results than in comparison to CPMD results. The end to end results support the presence of an open conformation in aqueous solution as well as a closed conformation in gas phase and partially closed conformation in chloroform solvent. The modified N14 and C3 atom distance and hydrogen bonding pattern in aqueous solution are useful in understanding of spontaneous proton transfer process in asparagine.

3.2. One-Fold Potential Energy Barriers and Dependency of Dipole Moments. One-fold potential energy barriers and the dependency of the dipole moment with respect to torsional angles are presented in Figures 6 and 7. The rotational

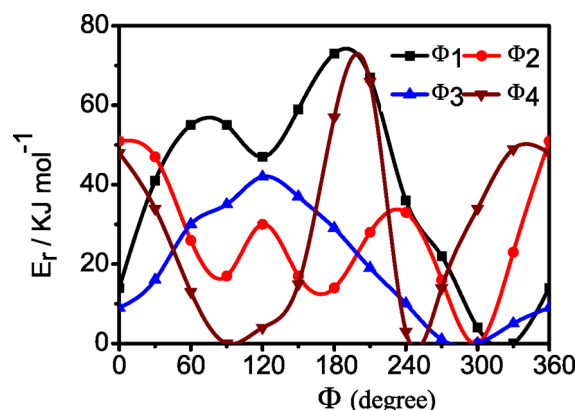


Figure 6. Relaxed-rotational barriers related to torsion angles ϕ_1 , ϕ_2 , ϕ_3 , and ϕ_4 of asparagine (MP2 method).

charged atoms were found at a distance less than 4 Å in both CPMD and MD simulations, which is in agreement with X-ray structure experimental investigations of glycine proteins.^{66–69} It concludes that intramolecular interaction in asparagine is also stabilized by interactions of opposite dipoles between side chain and terminal carbonyl groups, which is not changed with solvent polarity. The distribution of end to end distance values

barriers along four torsional conformational degrees of freedom, namely, Φ_1 (O1–C3–C5–C10), Φ_2 (C3–C5–C10–C13), Φ_3 (C5–C10–C13–N14), and Φ_4 (C3–C5–N6–H7), indicate large rigidity of asparagine. The rotational barrier around (C–C) bond with respect to (Φ_1), (Φ_2), and (Φ_3) are about 70, 50, and 40 kJ/mol, respectively, and the rotational barrier around (C–N) bond with respect to (Φ_4) is about 70 kJ/mol. In (Φ_2) and (Φ_3), torsional rotational

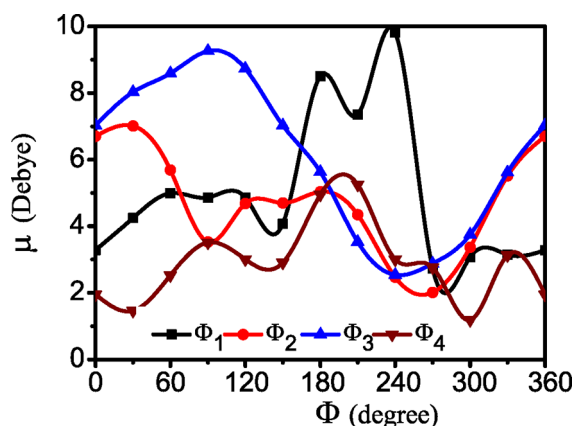


Figure 7. Dependency of dipole moment related to torsion angles ϕ_1 , ϕ_2 , ϕ_3 , and ϕ_4 of asparagine (MP2 method).

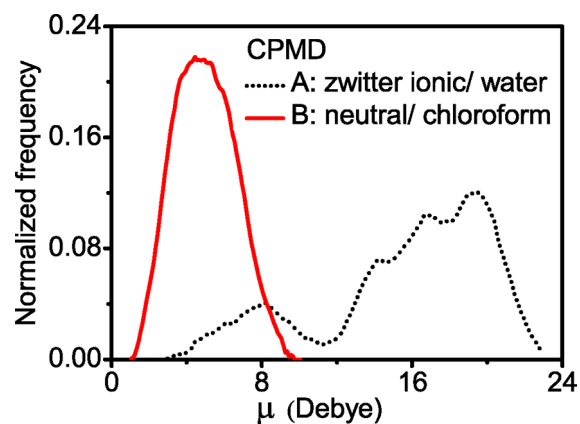


Figure 8. Dipole moment distribution of asparagine in water and chloroform solvents from CPMD simulations.

barriers conformers with the corresponding torsion angle value of 300° show an energy minimum (-491.1307 hartree) of asparagine, which are gauche-like conformers, and the conformers with respect to torsional angles (Φ_1) and (Φ_4) also show the same energy minimum in 330° and 90° , respectively, which is the global energy minimum of asparagine. These most stable conformers slightly differ in their dipole moment values, and barriers differ with respect to the number of local energy minimum. The rotational barriers around (C–C) and (C–N) both show the same level of rigidity in asparagine. The conformation-dependent polarity of asparagine is estimated by calculating the dipole moment as a function of torsion angles. The larger dependency of dipole moment values around 3 to 10 D was observed with respect to torsion angle Φ_1 , and smaller variation was observed in other torsion angles. The intramolecular hydrogen bondings, such as ($-\text{OH}\cdots\text{O}=\text{C}$) and ($-\text{OH}\cdots\text{NH}_2$), and similar orientations of the terminal and side chain carbonyl groups contribute larger dipole moment values of the rotamers.

3.3. Solvent Polarity-Dependent Tautomeric Shift and Dipole Moment Distribution of Asparagine. The solvent polarity has an important effect on preferred neutral to zwitterionic isomers of asparagine. In all simulations of asparagine in different environments, we used the neutral form of asparagine as a starting structure and found the molecular conformation to remain in the neutral form for both vacuum and chloroform solvent. However, in the case of aqueous solution, we observed a spontaneous proton transfer from the terminal carboxyl group to the terminal amino group leading to a tautomeric transition to a zwitterionic form. This observation indicates that the neutral form of asparagine is more stable in gas phase and in chloroform solvent, while the zwitterionic form is the most stable form in aqueous solution. This is in agreement with Raman spectroscopy results of asparagine in aqueous solution,^{27,28} which suggest a zwitterionic form of asparagine in aqueous solution. We have also computed the dipole moment distribution of asparagine in chloroform and aqueous solution, and the results are shown in Figure 8, where the molecular dipole moment refers to the first moment of the charge distribution. The charges are obtained as best fitting to the molecular electrostatic potential. The charges are generally referred as D-RESP charges⁷⁰ and are dynamically generated electrostatic potential quantities in the CPMD simulations, which depend on the instantaneous electric field generated by the dynamic solvent environment. The charges

and molecular dipole moments serve as indicators for the dielectric nature of the environment. A more polar solvent environment polarizes asparagine to a larger extent, and it exhibits larger net atomic charges and molecular dipole moments in such a condition.

Interestingly, the dipole moment distribution for asparagine in aqueous solution has a bimodal nature where the first distribution corresponds to neutral and latter one to zwitterionic form. The dipole moment of the neutral isomer is two times larger in water solvent than in chloroform. In a similar manner, the zwitterionic isomer shows a three times larger dipole moment (20 D) than its neutral isomer in aqueous solution. Probably such a high dipole moment of zwitterionic isomers increases its stability in aqueous solution through solute–solvent and dipole–dipole interactions. However, in the gas phase, the neutral isomer is more stable because this form has a stronger stabilization resulting from a large number of intramolecular hydrogen bondings.

The D-RESP charges for all the heavy atoms of asparagine in chloroform and aqueous solution are presented in Figure 9. The electron density ρ corresponds to $-q/\text{D-RESP}$. The huge impact on D-RESP charges of the C3 and O1 atoms observed, which is due to formation of α -carbanion, in the former one, a sign is changed, and in the later one, a high increment observed. For atoms N6, O17, and O4, larger D-RESP values are

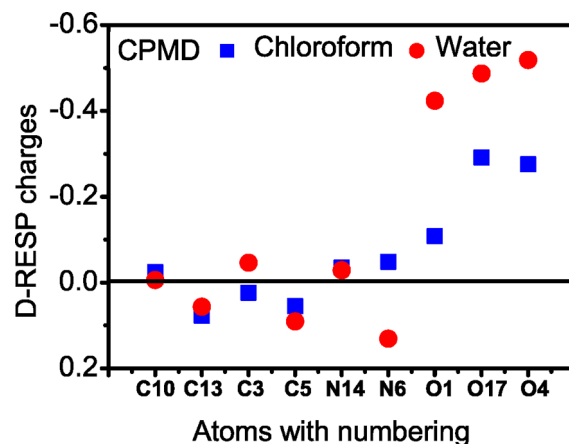


Figure 9. Dynamically restrained electrostatic potential (D-RESP) charges on heavy atoms of asparagine in chloroform and water solvents from CPMD simulations.

observed, but there is no change in the values of C5, C10, C13, and N14 atoms even in aqueous solution. The altered D-RESP charge distribution on O1 and N6 in aqueous solution favors the spontaneous proton transfer from the terminal carboxyl to the amino group, which results in a further change in the D-RESP charges on these atoms.

Overall, in a solvent medium with no or small solvent polarity, the asparagine stabilization occurs through beneficial intramolecular interactions, while, in a polar solvent, the stabilization energy has contributions from both intra- and intermolecular interactions. On the basis of this argument, it appears that the solute–solvent interaction energy (that contributes predominantly to the solvation free energy) dictates the nature of the conformation in a particular solvent medium. To understand the influence of this interaction energy over intramolecular energy, MP2 level of static calculations were performed on neutral, zwitterionic, and transition states of asparagine in PCM model of solvents, where the solvents are associated with increasing dielectric constant (ϵ) values. The solvents considered in this study are chloroform ($\epsilon = 4.7113$), *o*-nitro toluene ($\epsilon = 25.669$), acetonitrile ($\epsilon = 35.688$), dimethyl sulphoxide ($\epsilon = 46.826$), water ($\epsilon = 78.3553$), and formamide ($\epsilon = 108.94$), which cover a range of dielectric constants between 4.7 to 108.9. Interestingly, we found that the zwitterionic isomer of asparagine is more stable than the neutral isomer in water, which appears to be an energy minimum. The relative energetics of neutral, zwitterionic, and transition states of asparagine were calculated with respect to the zwitterionic isomer of asparagine in aqueous solution. The relative energy of such three different states of asparagine in different solvents were given as a function of solvent dielectric constant in Figure 10. As it can be seen, the energy of the zwitterionic isomer

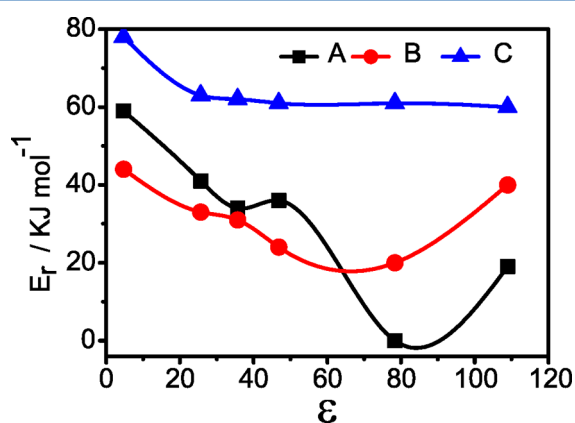


Figure 10. Correlation between relative energy of (A, zwitterionic; B, neutral; C, transition state) isomers with dielectric constants of solvents.

becomes lower than the neutral isomer for the solvent polarity range between DMSO and water. Therefore, it appears that the shift toward the zwitterionic isomer for and above the dielectric constant corresponding to that of the DMSO solvent. The flat energy curve of the transition state in different solvents indicates that the PCM model solvation energy has not changed energy for the transition state to any appreciable extent.

4. CONCLUSIONS

The closed conformation of asparagine obtained from gas phase CPMD and MD simulations. A strong cage-effect is shown for asparagine in aqueous solution, which is weaker or nonexistent in chloroform solvent and results in open conformations of asparagine in aqueous solution. The transformation from the neutral to the zwitterionic isomer of asparagine was observed in aqueous solution. Both gas phase and solution phase theoretical simulation results are in agreement with the corresponding experimental results. It concludes that intermolecular hydrogen bondings have strong influence over intramolecular hydrogen bondings in aqueous solution of asparagine, which leads to conformational unlocking of asparagine. Static quantum mechanical calculations with respect to torsion angle(Φ 1) show larger rigidity and polarity of asparagine, and PCM solvent calculations indicate that a shift from neutral to the most stable zwitterionic isomer of asparagine occurs in between DMSO and water solvents.

■ ASSOCIATED CONTENT

Supporting Information

Conformers related to different torsion angles. This material is available free of charge via the Internet at <http://pubs.acs.org>.

■ AUTHOR INFORMATION

Corresponding Author

*E-mail: agren@theochem.kth.se (H.A.); murugan@theochem.kth.se (N.A.M.); arkrishnan@theochem.kth.se (A.R.K.S.).

Notes

The authors declare no competing financial interest.

■ ACKNOWLEDGMENTS

This work was supported by a grant from the Swedish National Infrastructure Committee (SNIC) for the project “Multiscale Modeling of Molecular Materials” SNIC 023/07-18.

■ REFERENCES

- (1) Robinson, A. B.; McKerrow, J. H.; Cray, P. *Proc. Natl. Acad. Sci. U.S.A.* **1970**, *66*, 753–757.
- (2) Kainosho, M.; Ajisaka, K. *J. Am. Chem. Soc.* **1975**, *97*, 5630–5631.
- (3) Abbadi, A.; Mcharfi, M.; Aubry, A.; Premilat, S.; Boussard, G.; Marraud, M. *J. Am. Chem. Soc.* **1991**, *113*, 2729–2735.
- (4) Imperiali, B.; Shannon, K. L.; Rickert, K. W. *J. Am. Chem. Soc.* **1992**, *114*, 7942–7944.
- (5) Robinson, N. E.; Robinson, A. B. *Proc. Natl. Acad. Sci. U.S.A.* **2001**, *98*, 944–949.
- (6) Li, C.; Thompson, C. B. *Science* **2002**, *298*, 1346–1347.
- (7) Deverman, B. E.; Cook, B. L.; Manson, S. R.; Neiderhoff, R. A.; Langer, E. M.; Rosova, I.; Kulans, L. A.; Fu, X.; Weinberg, J. S.; Heinecke, J. W.; Roth, K. A.; Weintraub, S. J. *Cell* **2002**, *111*, 51–62.
- (8) Nilsson, M. R.; Driscoll, M.; Raleigh, D. P. *Protein Sci.* **2002**, *11*, 342–349.
- (9) Goldberg, A. L. *Nature* **2003**, *426*, 895–899.
- (10) Li, B.; Borchardt, R. T.; Topp, E. M.; VanderVelde, D.; Schowen, R. L. *J. Am. Chem. Soc.* **2003**, *125*, 11486–11487.
- (11) Reissner, K. J.; Aswad, D. W. *Cell. Mol. Life Sci.* **2003**, *60*, 1281–1295.
- (12) Weintraub, S. J.; Manson, S. R. *Mech. Ageing Dev.* **2004**, *125*, 255–257.
- (13) Zhao, R.; Yang, F. T.; Alexander, D. R. *Cancer Cell* **2004**, *5*, 37–49.
- (14) Huang, L.; Lu, J.; Wroblewski, V. J.; Beals, J. M.; Riggan, R. M. *Anal. Chem.* **2005**, *77*, 1432–1439.
- (15) Weintraub, S. J.; Deverman, B. E. *Sci. STKE* **2007**, *7*, 409–415.

- 444 (16) Lura, R.; Schirch, V. *Biochemistry* **1988**, *27*, 7671–7677.
- 445 (17) Patel, K.; Borchardt, R. T. *Pharm. Res.* **1990**, *7*, 703–711.
- 446 (18) Brennan, T. V.; Clarke, S. *Protein Sci.* **1993**, *2*, 331–338.
- 447 (19) Capasso, S.; Mazzarella, L.; Sica, F.; Zagari, A.; Salvadori, S. *J. Chem. Soc., Perkin Trans.* **1993**, *2*, 679–682.
- 448 (20) Li, R.; D'Souza, A. J.; Schowen, R. L.; Borchardt, R. T.; Topp, E. *M. J. Peptide Res.* **2000**, *56*, 326–334.
- 451 (21) Peters, B.; Trout, B. L. *Biochemistry* **2006**, *45*, 5384–5392.
- 452 (22) Radkiewicz, J. L.; Zipse, H.; Clarke, S.; Houk, K. N. *J. Am. Chem. Soc.* **1996**, *118*, 9148–9155.
- 454 (23) Antipas, A. S.; Vander Velde, D. G.; Jois, S. D. S.; Siahann, T.; Stella, V. J. *J. Pharm. Sci.* **2000**, *89*, 742–750.
- 456 (24) Wakankar, A. A.; Borchardt, R. T. *J. Pharm. Res.* **2006**, *95*, 2321–2336.
- 458 (25) Boeckx, B.; Maes, G. *Biophys. Chem.* **2012**, *165*–166, 62–73.
- 459 (26) Cabezas, C.; Varela, M.; Pena, I.; Mata, S.; Lopez, J. C.; Alonso, J. L. *Chem. Commun.* **2012**, *48*, 5934–5936.
- 461 (27) Casado, J.; Lopez Navarrete, J. T.; Ramirez, F. *J. Raman Spectrosc.* **1995**, *26*, 1003–1008.
- 463 (28) Lopez Navarrete, J. T.; Casado, J.; Hernandez, V.; Ramirez, F. *J. Raman Spectrosc.* **1997**, *28*, 501–509.
- 465 (29) Imperiali, B.; Shannon, K. L.; Unno, M.; Rickert, K. W. *J. Am. Chem. Soc.* **1992**, *114*, 7944–7945.
- 467 (30) Aleman, C.; Puiggali, J. *J. Phys. Chem.* **1997**, *101*, 3441–3446.
- 468 (31) Lopez Navarrete, J. T.; Casado, J.; Hernandez, V.; Ramirez, F. *J. Theor. Chem. Acc.* **1997**, *98*, 5–15.
- 470 (32) O'Connor, S. E.; Imperiali, B. *J. Am. Chem. Soc.* **1997**, *119*, 2295–2296.
- 472 (33) Arnold, W. D.; Sanders, L. K.; McMahon, M. T.; Volkov, A. V.; Wu, G.; Coppens, P.; Wilson, S. R.; Godbout, N.; Oldfield, E. *J. Am. Chem. Soc.* **2000**, *122*, 4708–4717.
- 475 (34) Aylin Konuklar, F.; Aviyente, V.; Sen, T. Z.; Bahar, I. *J. Mol. Model.* **2001**, *7*, 147–160.
- 477 (35) Kimura, T.; Matubayasi, N.; Sato, H.; Hirata, F.; Nakahara, M. *J. Phys. Chem. B* **2002**, *106*, 12336–12343.
- 479 (36) Aylin Konuklar, F.; Aviyente, V.; Ruiz Lopez, M. F. *J. Phys. Chem. A* **2002**, *106*, 11205–11214.
- 481 (37) Galano, A.; Alvarez-Idaboy, J. R.; Bravo-Perez, G.; Ruiz-Santoyo, M. E. *J. Mol. Struct.* **2002**, *617*, 77–86.
- 483 (38) Rassolian, M.; Chass, G. A.; Setiadi, D. H.; Csizmadia, I. G. *J. Mol. Struct.* **2003**, *666*, 273–278.
- 485 (39) Aylin, F.; Konuklar, S.; Aviyente, V. *Org. Biomol. Chem.* **2003**, *1*, 2290–2297.
- 487 (40) Chen, X.; Guo, C. *J. Mol. Struct.* **2004**, *682*, 73–82.
- 488 (41) Chen, M.; Huang, Z.; Lin, Z. *J. Mol. Struct.* **2005**, *719*, 153–158.
- 489 (42) Kaliman, I.; Nemukhin, A.; Varfolomeev, S. *J. Chem. Theor. Comput.* **2010**, *6*, 184–189.
- 491 (43) Deane, C. M.; Allen, F. H.; Taylor, R.; Blundell, T. L. *Protein Eng.* **1992**, *12*, 1025–1028.
- 493 (44) Case, D. A.; et al. *AMBER11*; University of California: San Francisco, CA, 2002.
- 495 (45) Jakalian, A.; Bush, B. L.; Jack, D. B.; Bayly, C. L. *J. Comput. Chem.* **2002**, *21*, 132–146.
- 497 (46) Frisch, M. J.; et al. *Gaussian 09*, revision XXX; Gaussian, Inc.: Wallingford CT, 2009.
- 499 (47) Monecke, P.; Friedemann, R.; Naumann, S.; Csuk, R. *J. Mol. Model.* **1998**, *4*, 395–404.
- 501 (48) Friedemann, R.; Naumann, S.; Brickmann, J. *Phys. Chem. Chem. Phys.* **2001**, *3*, 4195–4199.
- 503 (49) Selvaraj, A. R. K.; Weissflog, W.; Pelzl, G.; Diele, S.; Kresse, H.; Vakhovskaya, Z.; Friedemann, R. *Phys. Chem. Chem. Phys.* **2006**, *8*, 1170–1177.
- 506 (50) Selvaraj, A. R. K.; Weissflog, W.; Friedemann, R. *J. Mol. Model.* **2007**, *13*, 907–917.
- 508 (51) Arul Murugan, N.; Hugosson, H. W. *Phys. Chem. Chem. Phys.* **2008**, *10*, 6135–6143.
- 510 (52) Arul Murugan, N.; Jha, P. C.; Agren, H. *Phys. Chem. Chem. Phys.* **2009**, *11*, 6482–6489.
- (53) Arul Murugan, N.; Hugosson, H. W. *J. Phys. Chem. B* **2009**, *113* (4), 1012–1021.
- (54) Selvaraj, A. R. K.; Hayase, H. *J. Mol. Model.* **2012**, *18*, 2099–2014.
- (55) Hutter, J.; et al. *CPMD version 3.11*; IBM Corp. and MPI-FKF: Stuttgart, Germany, 2012.
- (56) van Gunsteren, W. F.; Billeter, S. R.; Eising, A. A.; Hnenberger, P. H.; Krger, P.; Mark, A. E.; Scott, W. R. P.; Tironi, I. G. *Biomolecular Simulation: The GROMOS96 Manual and User Guide*; Vdf Hochschulverlag AG an der ETH Zurich: Zurich, Switzerland, 1996.
- (57) Laio, C.; VandeVondele, J.; Rthlisberger, U. *J. Chem. Phys.* **2002**, *116*, 6941–6947.
- (58) Warshel, A.; Levit, M. *J. Mol. Biol.* **1976**, *103*, 227–249.
- (59) Field, M. J.; Bash, P. A.; Karplus, M. *J. Comput. Chem.* **1990**, *11*, 700–733.
- (60) Becke, A. D. *Phys. Rev. A* **1988**, *38*, 3098–3100.
- (61) Lee, C.; Yang, W.; Parr, R. C. *Phys. Rev. B* **1988**, *37*, 785–789.
- (62) Trouiller, N.; Martin, J. L. *Phys. Rev. B* **1991**, *43*, 1993–2006.
- (63) Head-Gordon, M.; Pople, J. A.; Frisch, M. J. *J. Chem. Phys. Lett.* **1988**, *153*, 503–506.
- (64) Peng, C.; Schlegel, H. B. *Isr. J. Chem.* **1993**, *33*, 449–454.
- (65) Peng, C.; Ayala, P. Y.; Schlegel, H. B.; Frisch, M. J. *J. Comput. Chem.* **1996**, *17*, 49–56.
- (66) Albrecht, G.; Corey, R. B. *J. Am. Chem. Soc.* **1939**, *61*, 1087–1103.
- (67) Jonsson, P.-G.; Kvick, A. *Acta Crystallogr., Sect. B: Struct. Sci.* **1972**, *28*, 1827–1833.
- (68) Jensen, J. H.; Gordon, M. S. *J. Am. Chem. Soc.* **1995**, *117*, 8159–8170.
- (69) Tortonda, F. R.; Pascual-Ahuir, J. L.; Silla, E.; Tunon, I. *Chem. Phys. Lett.* **1996**, *260*, 21–26.
- (70) Laio, A.; VandeVondele, J.; Rothlisberger, U. *J. Phys. Chem. B* **2002**, *106*, 7300–7307.